Integration of seismo-acoustic data

Nick Varley

PASI Costa Rica 2011

Applications

- Increasingly studies are integrating data from a variety of sources to improve:
  - Models of eruption mechanisms
  - Event forecasting
  - Hazard assessments
- Seismic data usually represents most continuous stream with highest sampling rate – increasingly being combined with infrasound data
- Other data sets
  - Ground-based thermal data
  - Remote sensing
  - Deformation
  - Gas emission

Volcán de Colima

- Current effusive eruption: Jan 2007 – now
- Daily small Vulcanian explosions
- Variable energy & ash-contents

Applications of seismic signals

- Event counting
  - Both automated and manual
- Event location
  - Lack of VT events
- Forecasting activity
  - Long-term - VT swarms
  - LP swarms as precursor
  - Determination of style – similar LP swarms prior to both effusive and explosive
- LP & tremor
  - Significance for evolution of activity
- Explosion generation mechanism
  - Variations in both waveform & spectrum. Time series analysis
- Lahar warning & characterization
- Rockfall signals – estimation of effusion rate

RESCO - Universidad de Colima

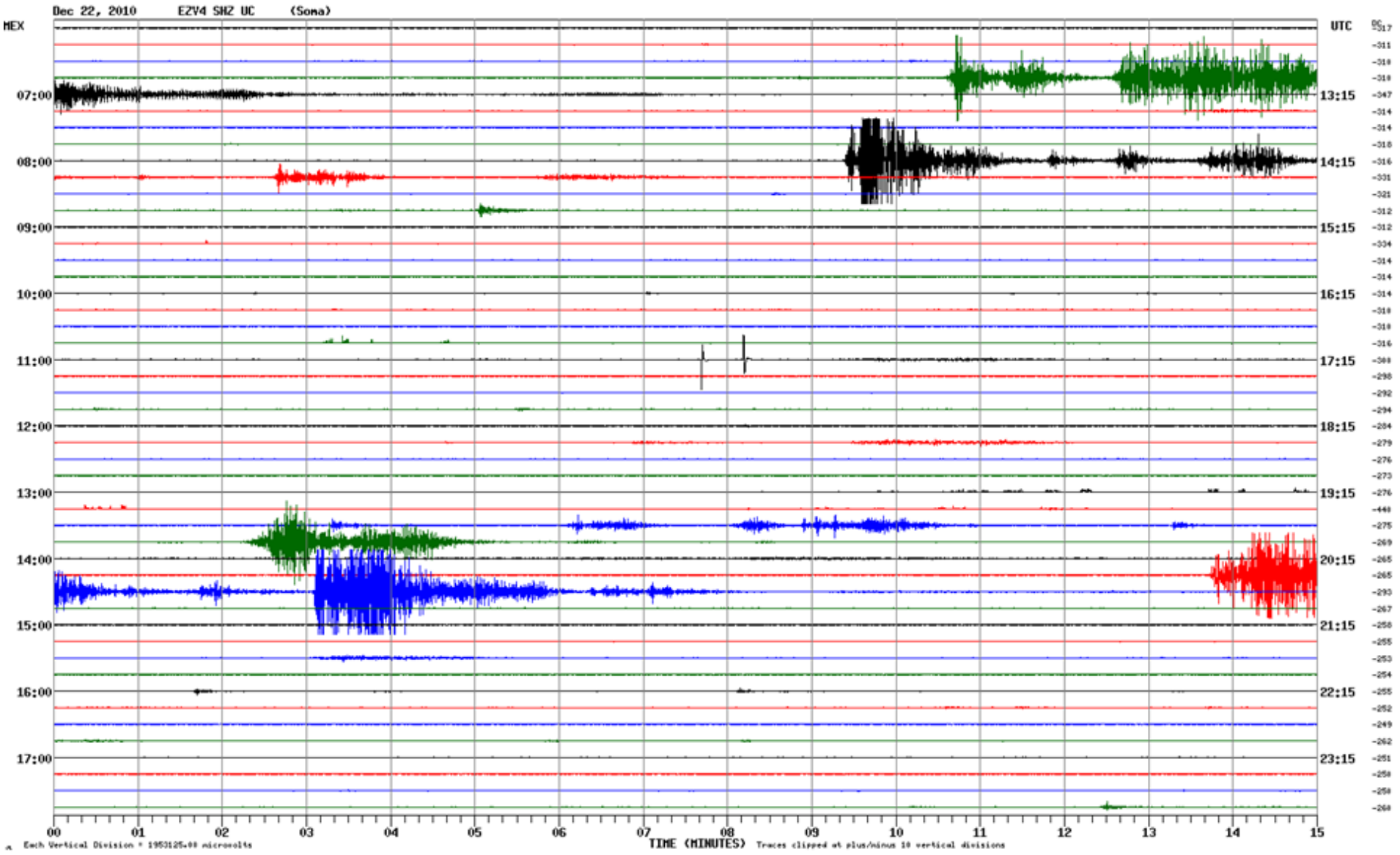

Swarms of LP events associated with larger Vulcanian events (2005)

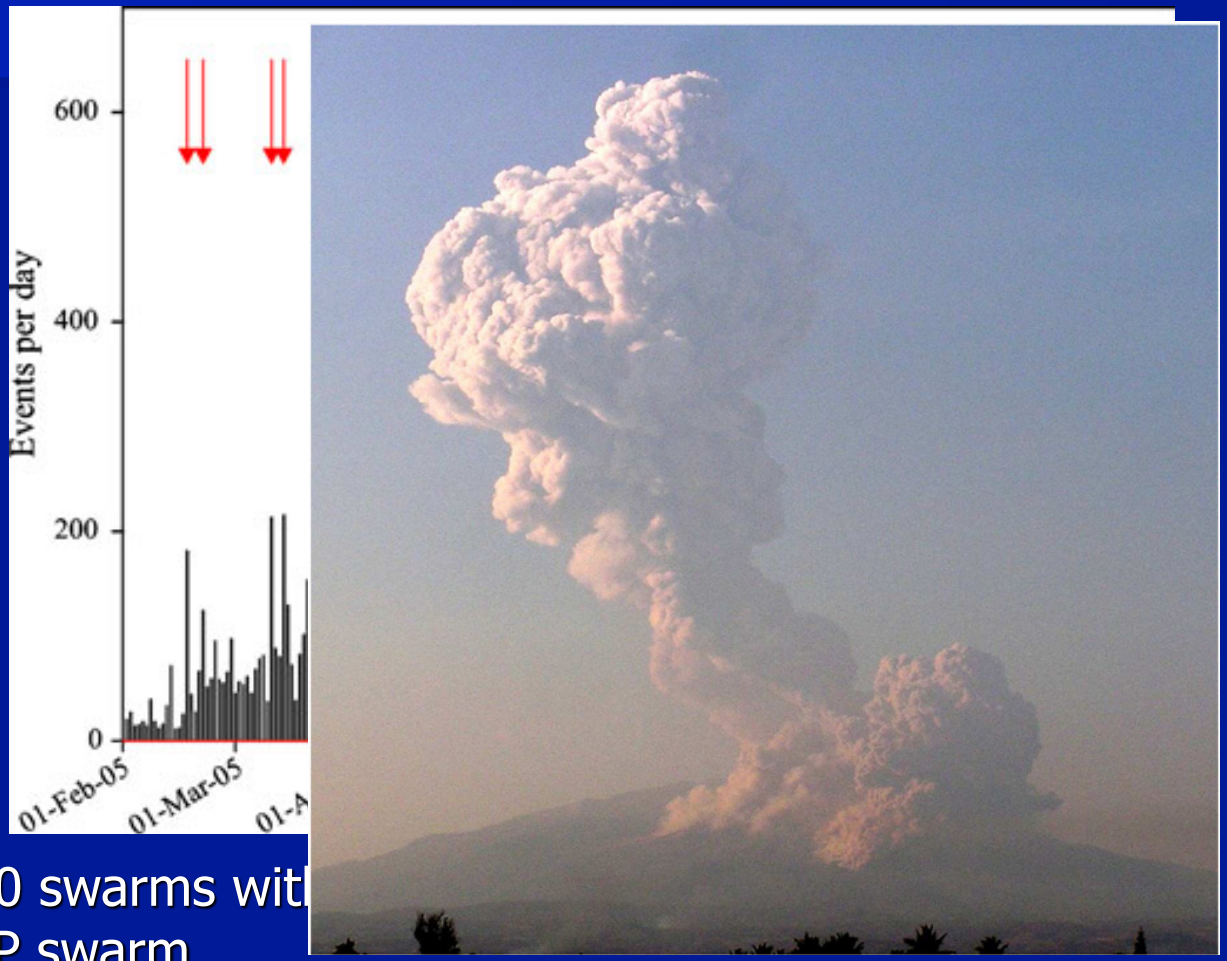

- 30 swarms wit
  LP swarm
- PFs to 5.4 km

13 – 16 Sept. 2005

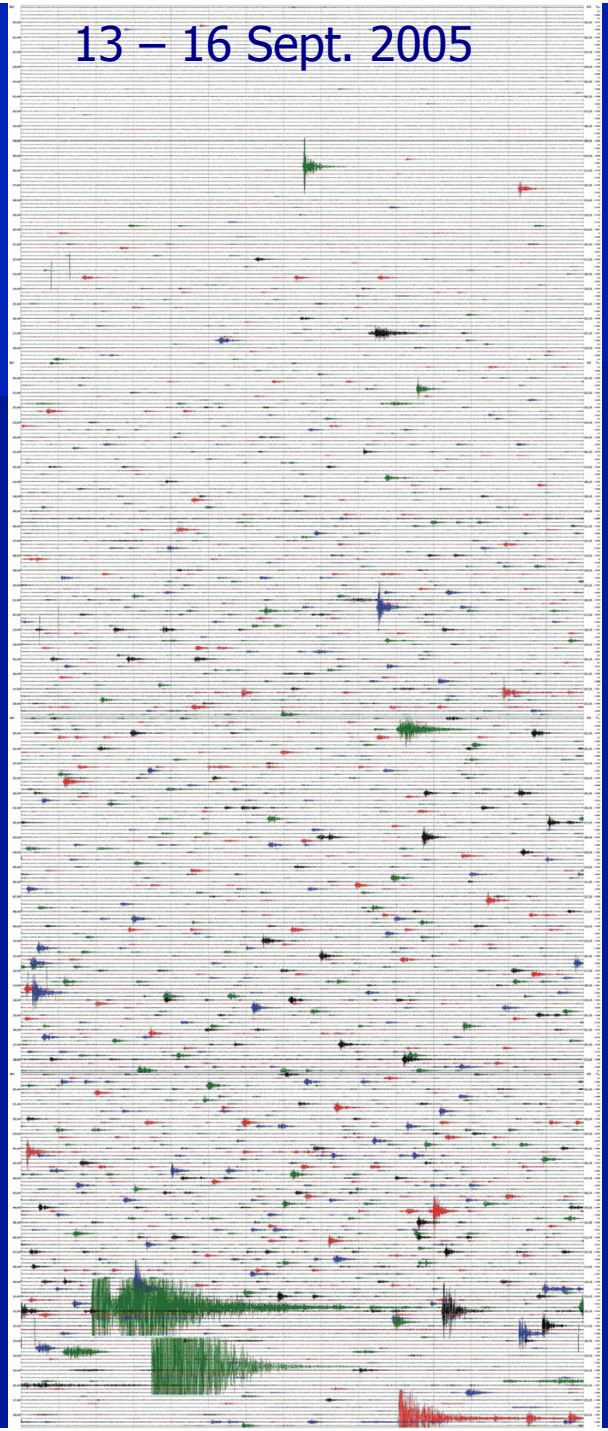

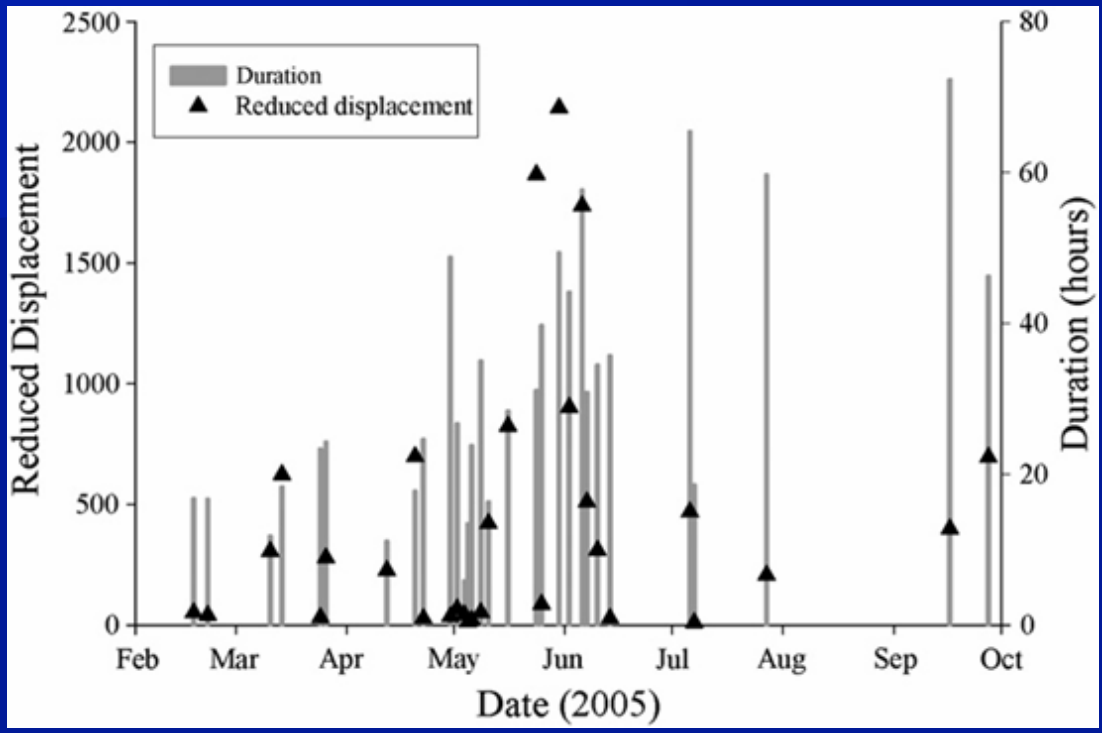

- Poor correlation between explosion size & swarm characteristics

Families of LP Events

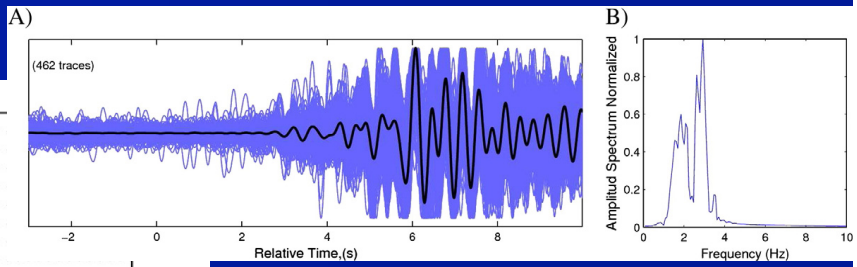

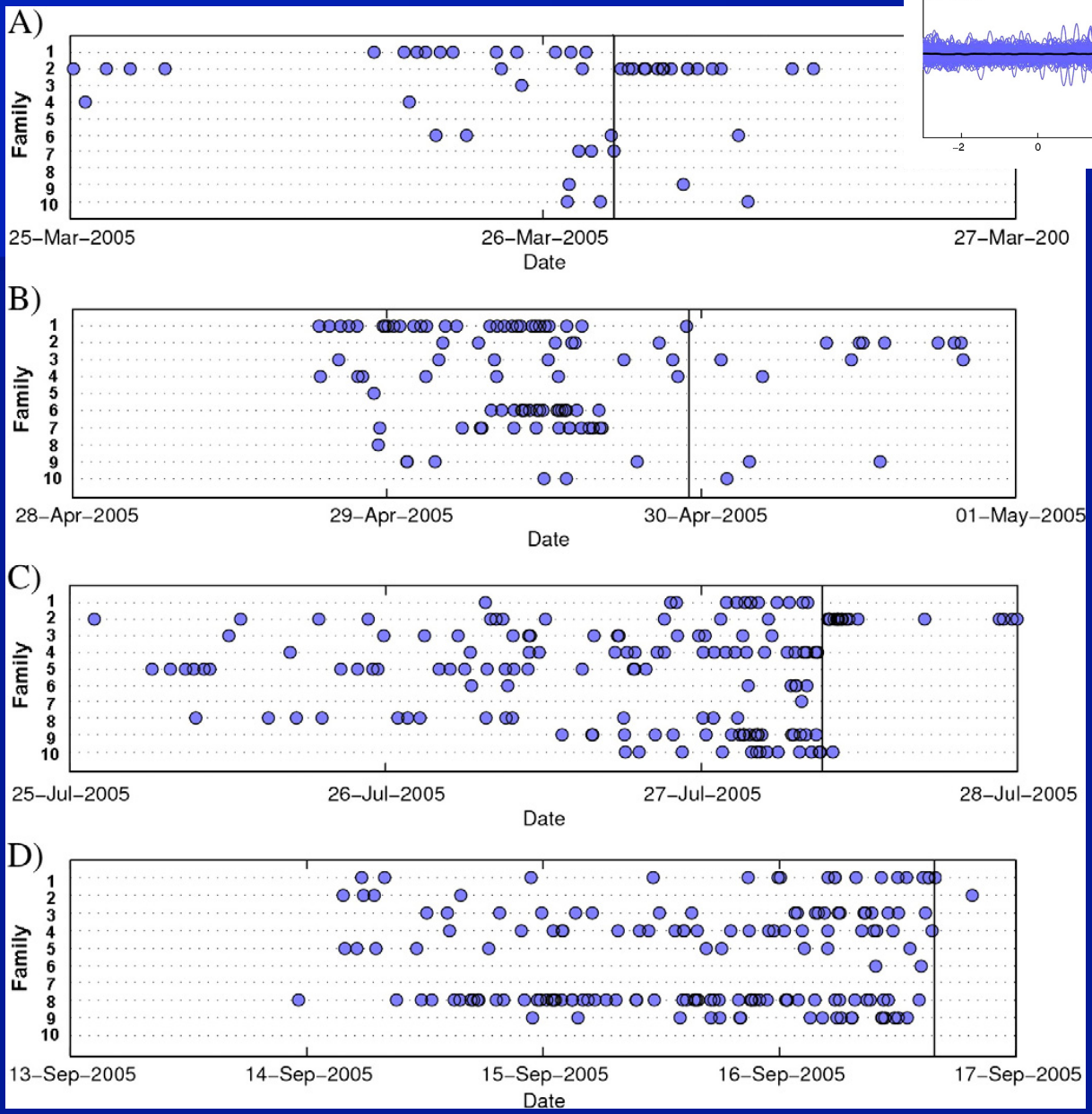

- Some families present only before or after explosion
- Families repeat in each swarm

Varley et al. JVGR 2010

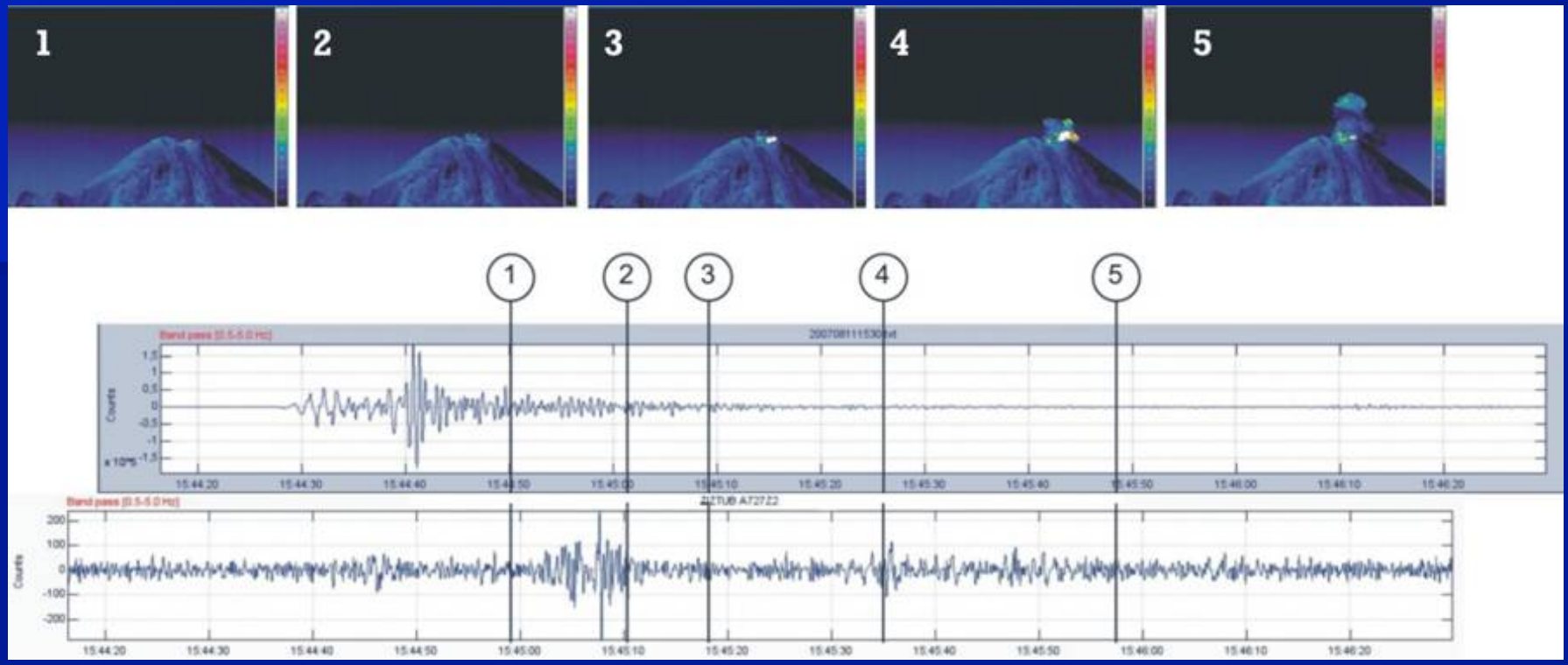

Explosion 11/08/07

Seismic signal – LF onset after rupture of impermeable plug, then fragmentation

2nd pulse produces acoustic emission but no seismicity detected

2 sources shown in thermal images – one rich in ash, the other poor

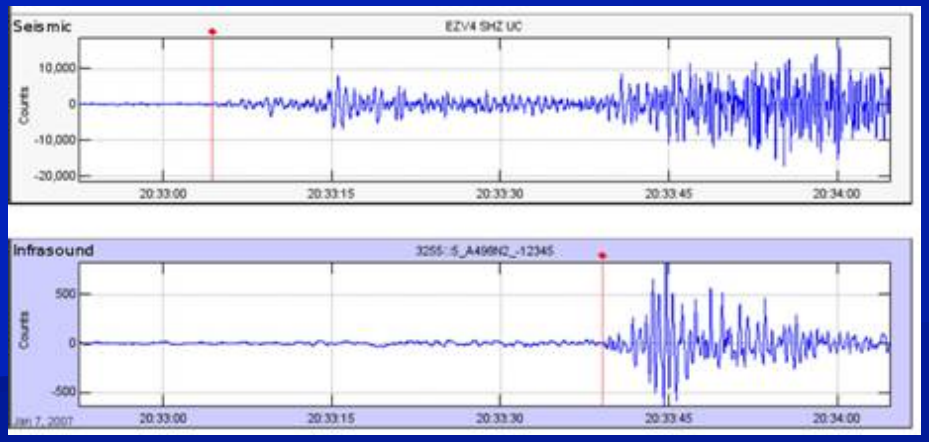

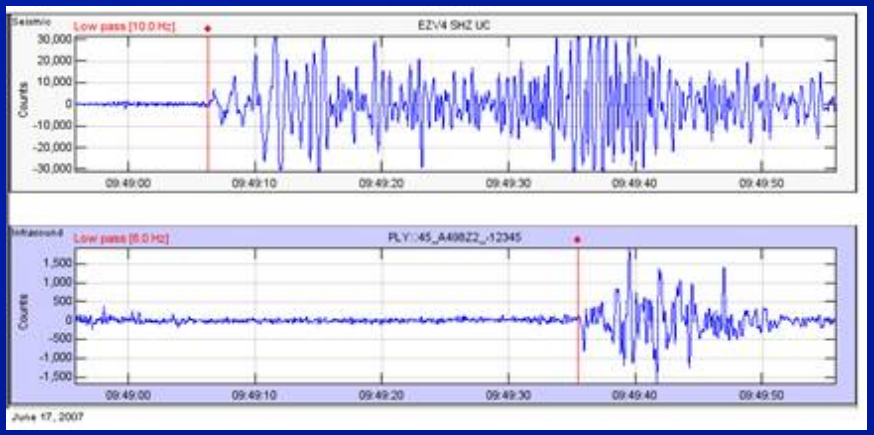

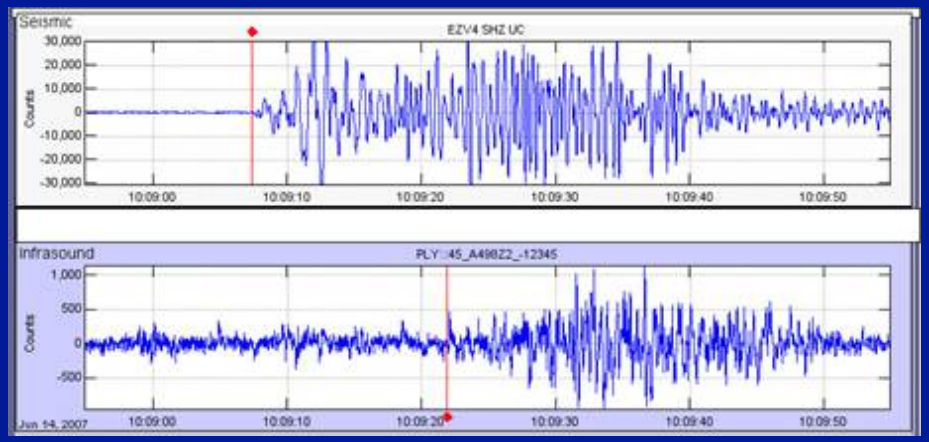

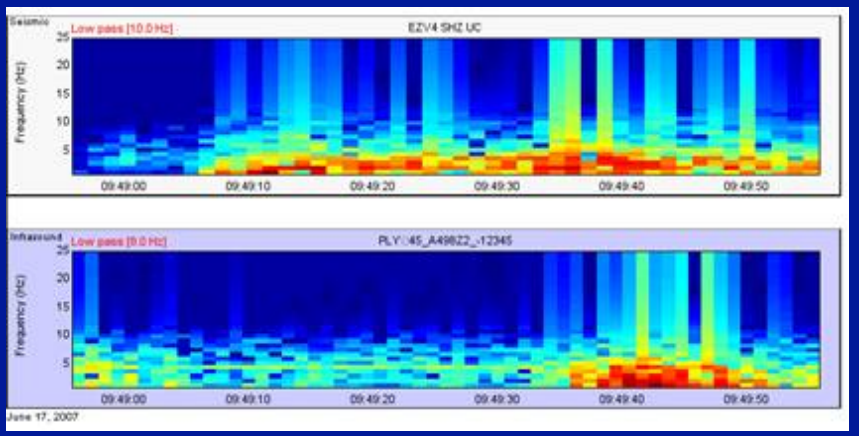

Infrasound analysis

- Comparison between onset of seismic & infrasound sign
- Energy partition
- Comparison with thermal emission & ascent rate
- Spectral comparison
- Increase in stations to 5 – identification of source vent
- Rockfall magnitude
- Infrasound v. gas release

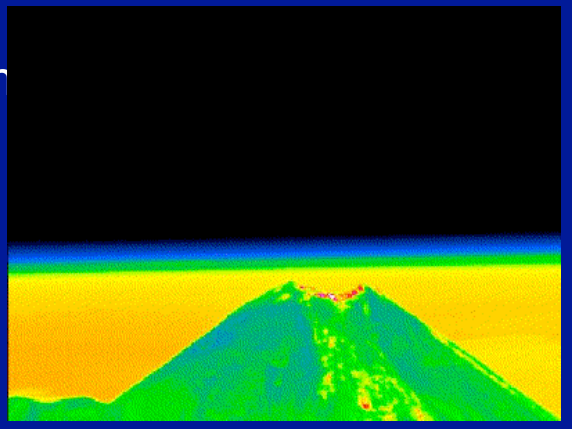

Event classification

- Neural networks – ~ 80% efficient (Vesuvius, Soufrière Hills, Villarrica)
  - Relies on good training
  - Only works with selected events not whole record
- Hidden Markov Chains
  - Developed for voice recognition
  - Also requires extensive training
  - Works for continuous record

Evolution of seismicity

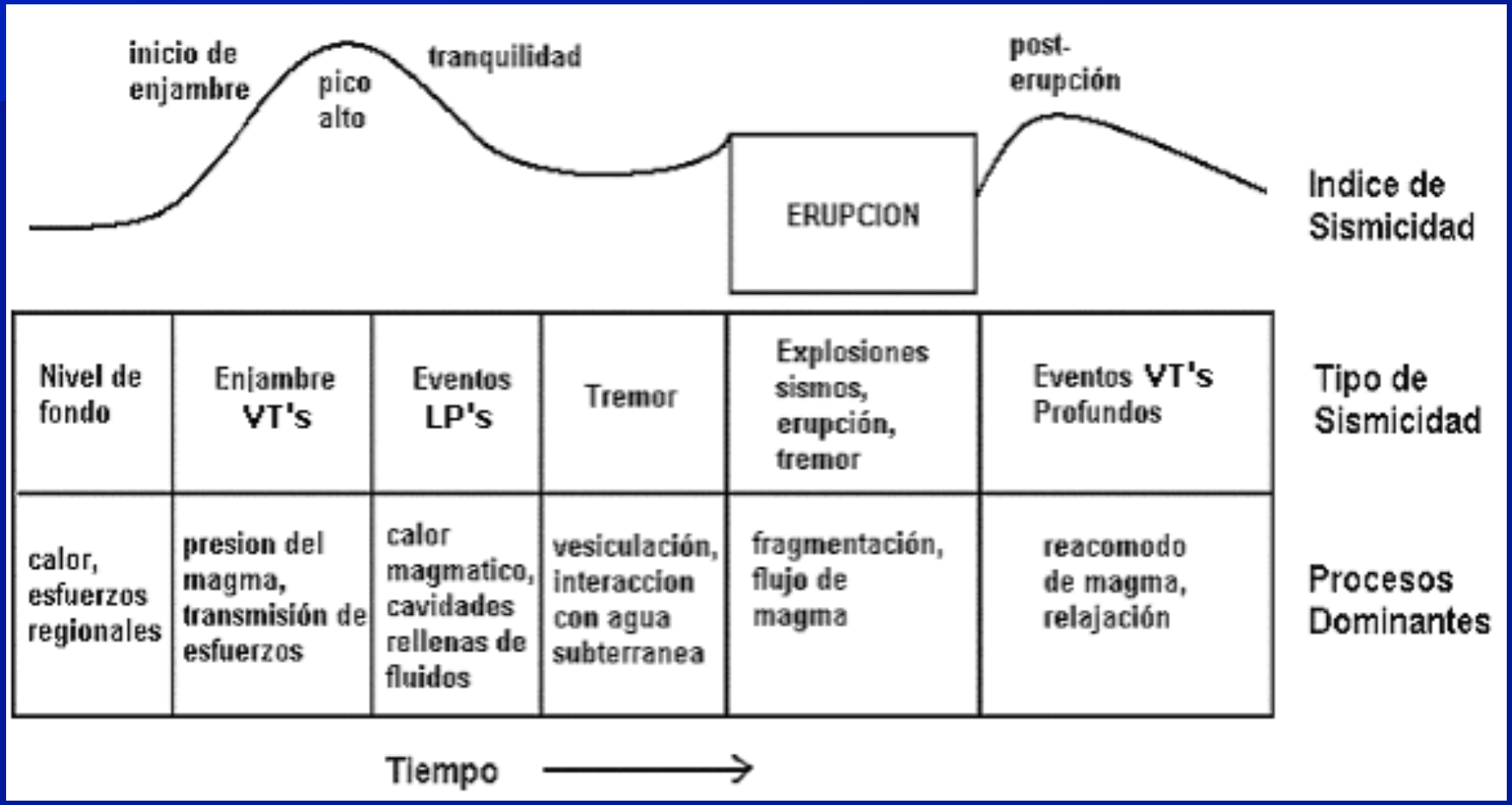

McNutt 1996

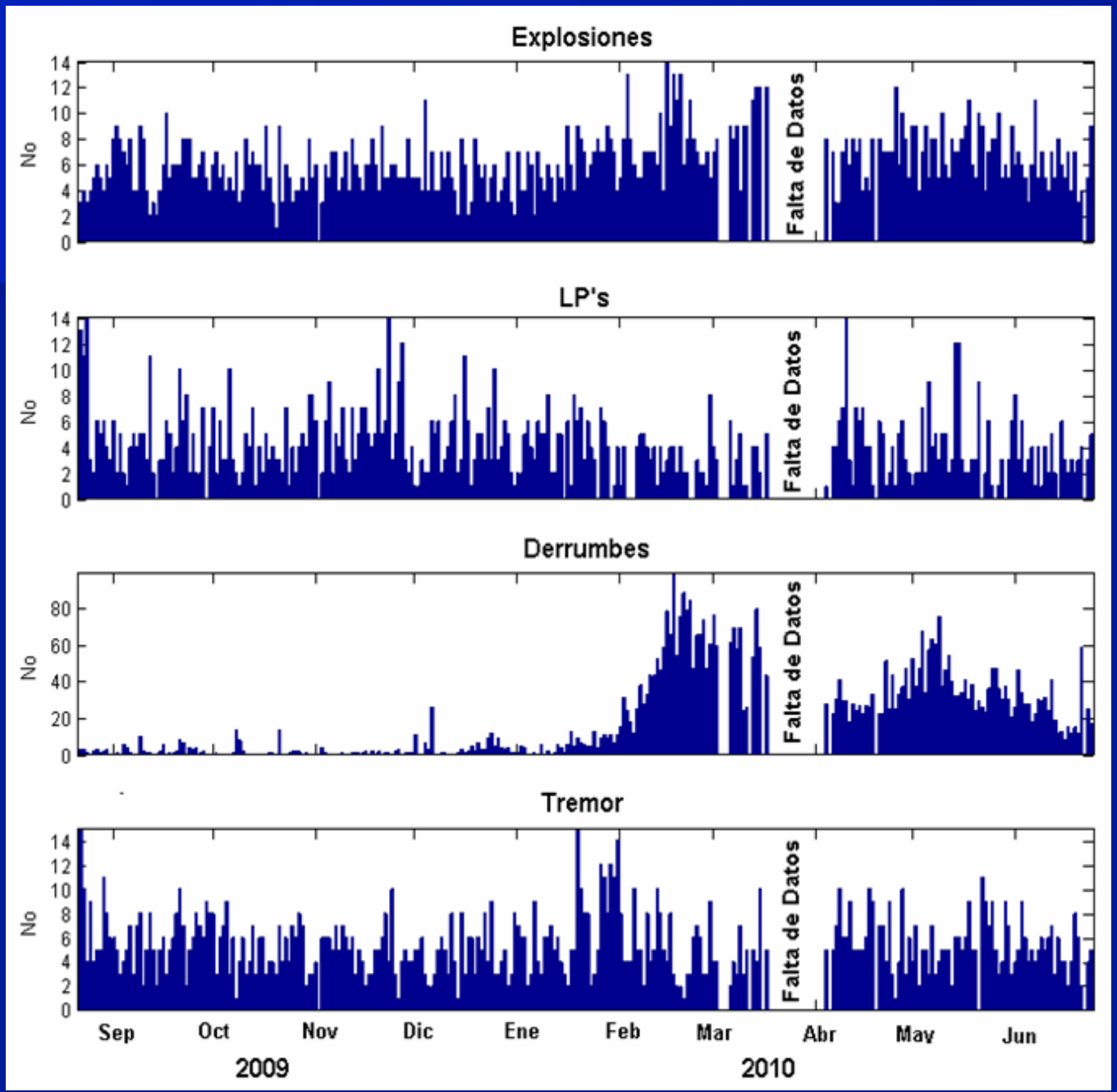

SOMA short-period station

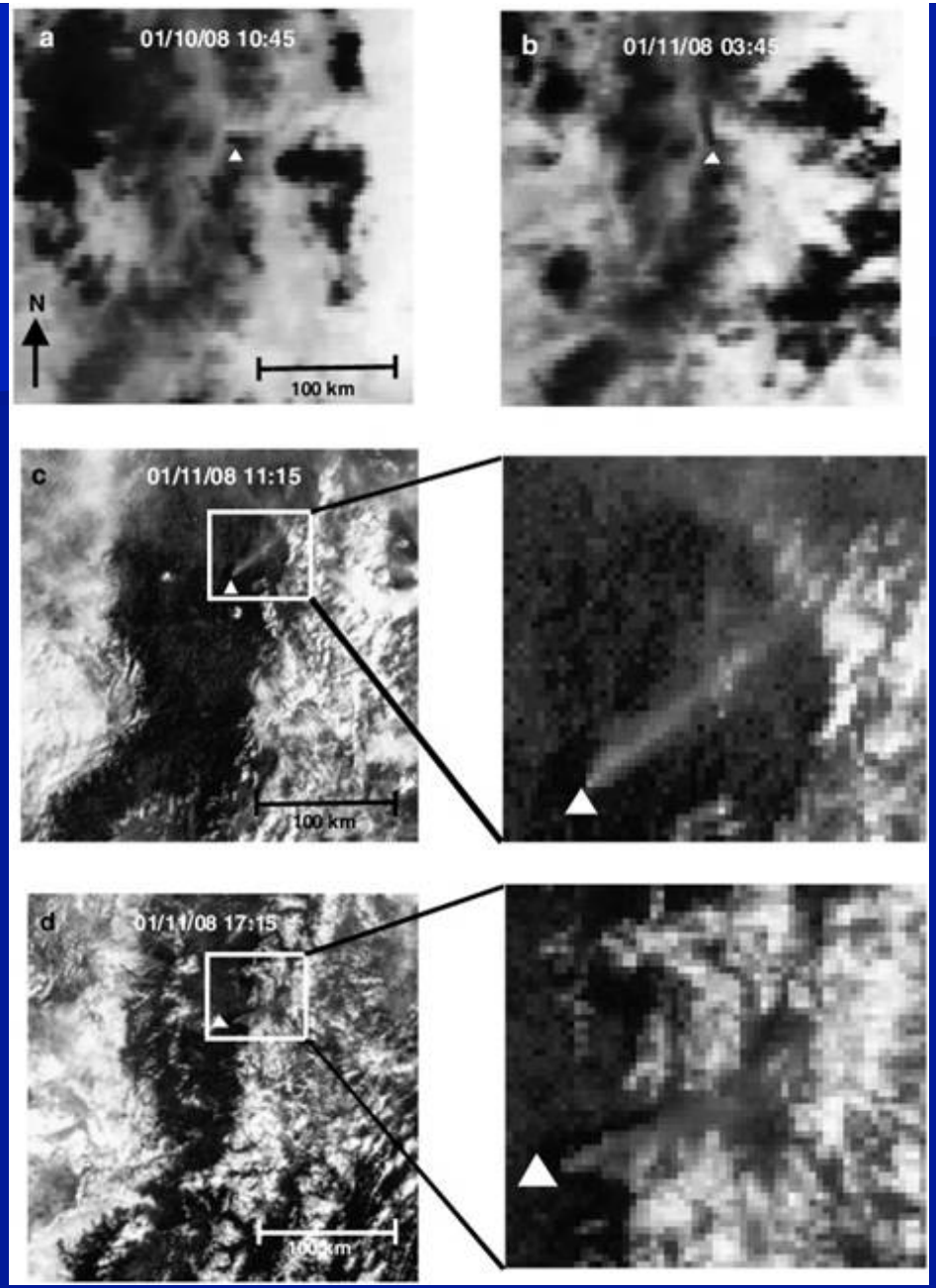

GOES imagery of January 2008 eruption sequence (both TIR & VIS).

Tungurahua

Integrating remote sensing techniques and infrasound

- Satellite- eruption chronologies, plume information: heights and aspect ratios
- Integrated with infrasound data and hand-held thermal imagery
- Aided identification of accurate eruption onsets, durations and cessations

Steffke, A.M. et al., 2010. JVGR, 193(3-4): 143-160.

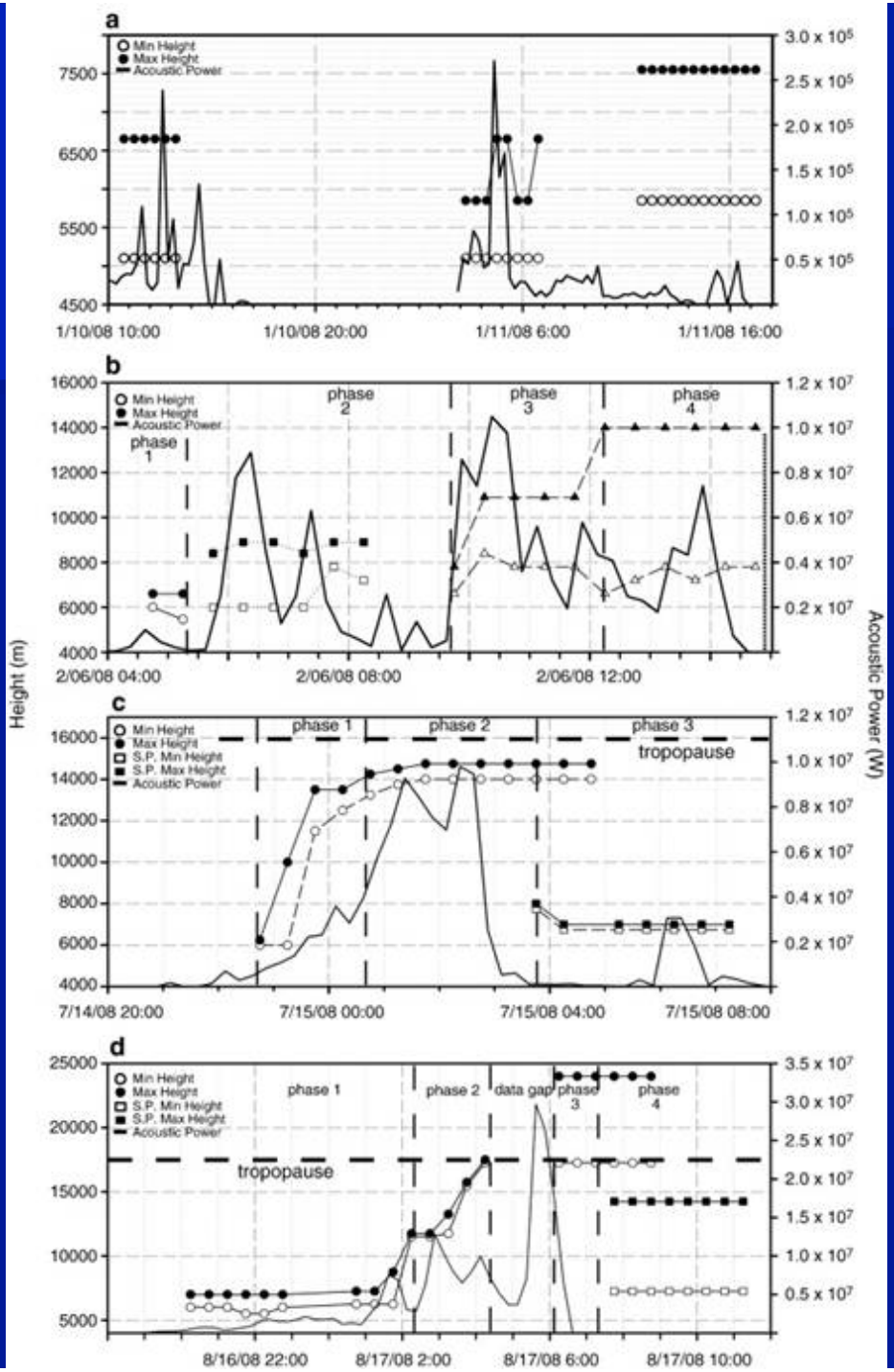

- Defined types of eruption styles ranging from plinian to weak vulcanian
- Results show a positive correlation between timing of plume height and acoustic power
- Good correlation is observed for maximum plume height and acoustic power for plinian (d) and sub-plinian (c) eruptions, with correlation for weaker eruptions decreased (a and b).

a) Sustained column

b) Collapsed and resulted in a series of PFs

c) August 2006 eruption - initially the eruption was less energetic, PFs

d) Energetic portion of the eruption with a large sustained column

e) As d)

f) Final image collected after the end of the eruption - warm PF deposits on flanks, with no activity at the summit

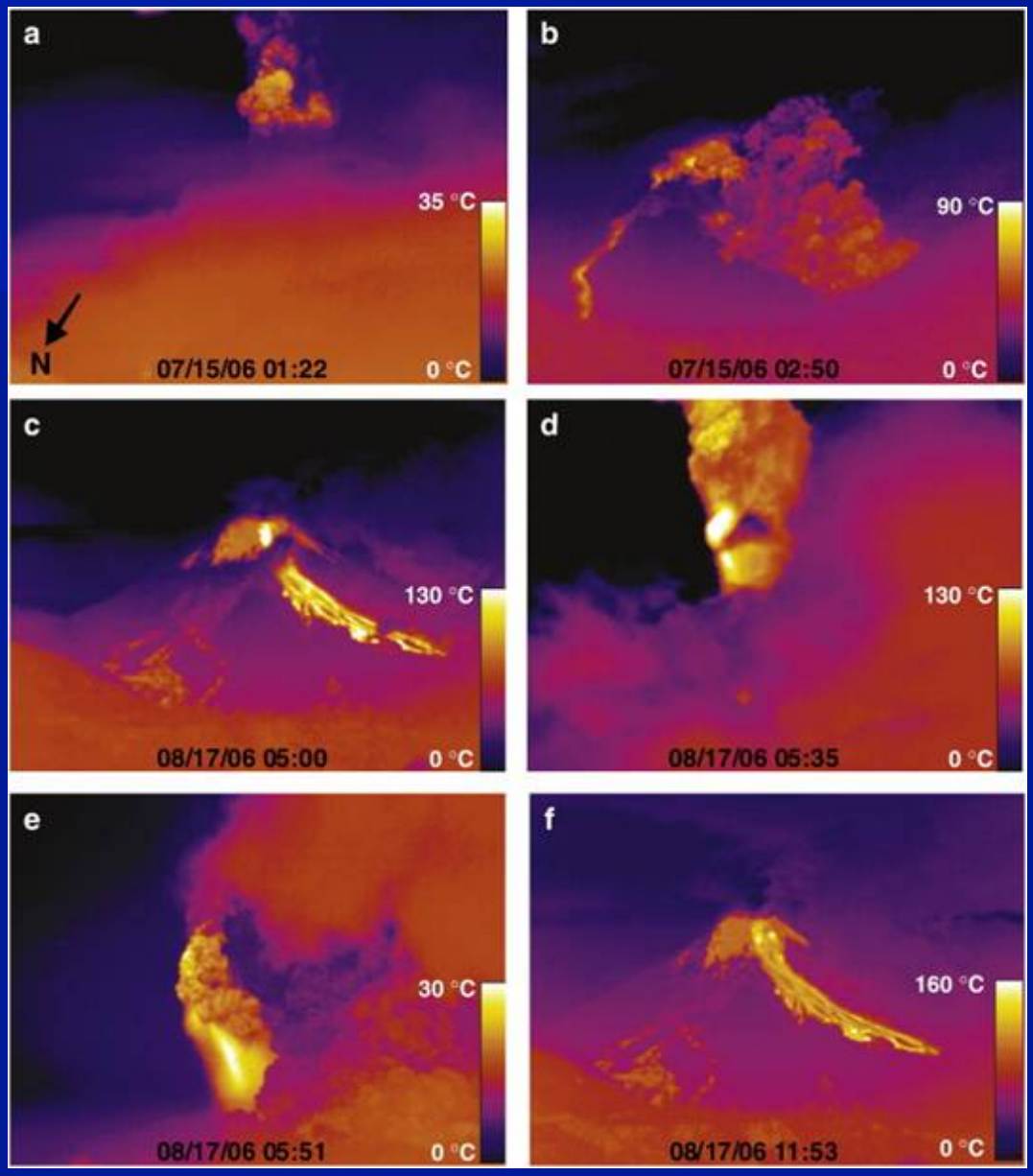

Infrared imagery of July and August 2006 eruptions

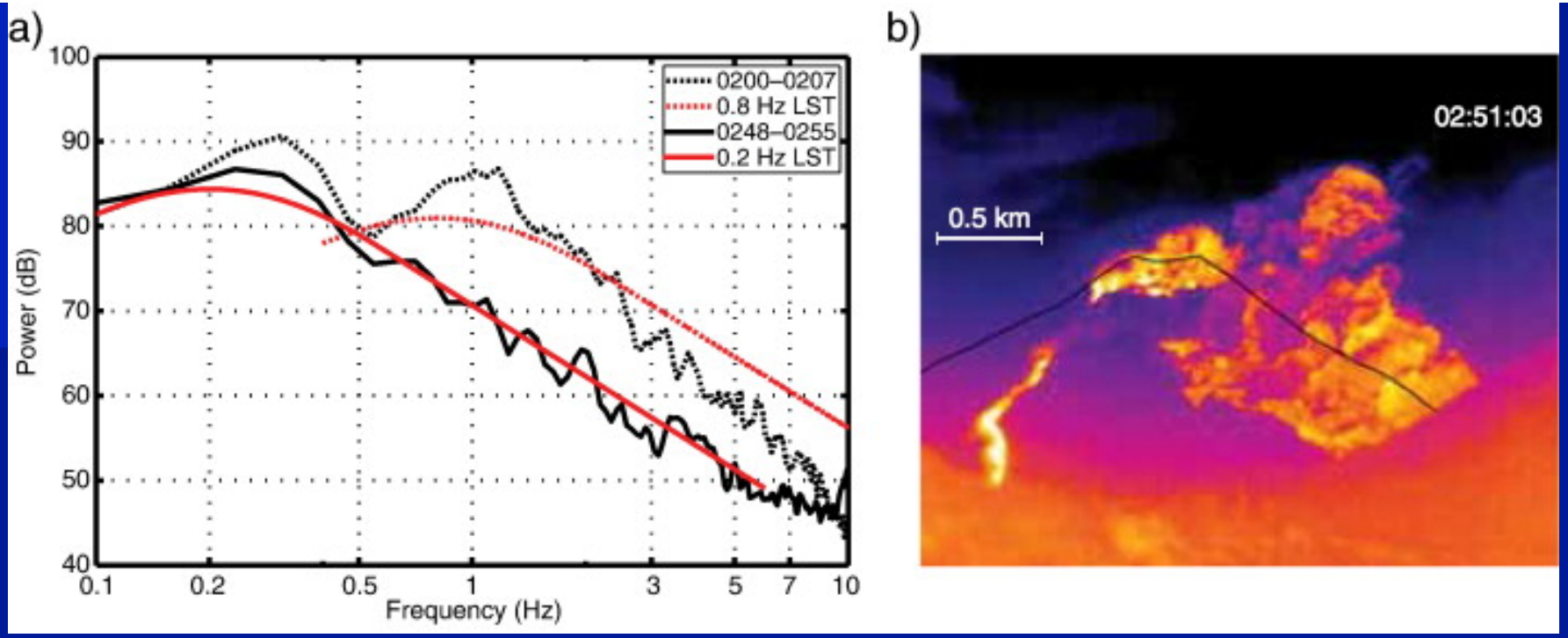

Fee, D. et al. 2010. JVGR, 193(1-2): 67-81.

Power spectral density comparison for sustained vs. collapsed columns (15 July 2006). Dashed black line - spectrum during a time period of sustained jetting with a vertical ash and gas column above the vent. Dark black line - spectrum during a period where the column has collapsed to feed PFs.

Note there is no "notch" in the spectrum for the PF period, only a single peak centred at ~ 0.25 Hz.

IR image from 15 July 15 02:51:03 UTC showing a large PF descending the volcano and no sustained vertical column. This time period coincides with the single-peaked spectrum (black line)

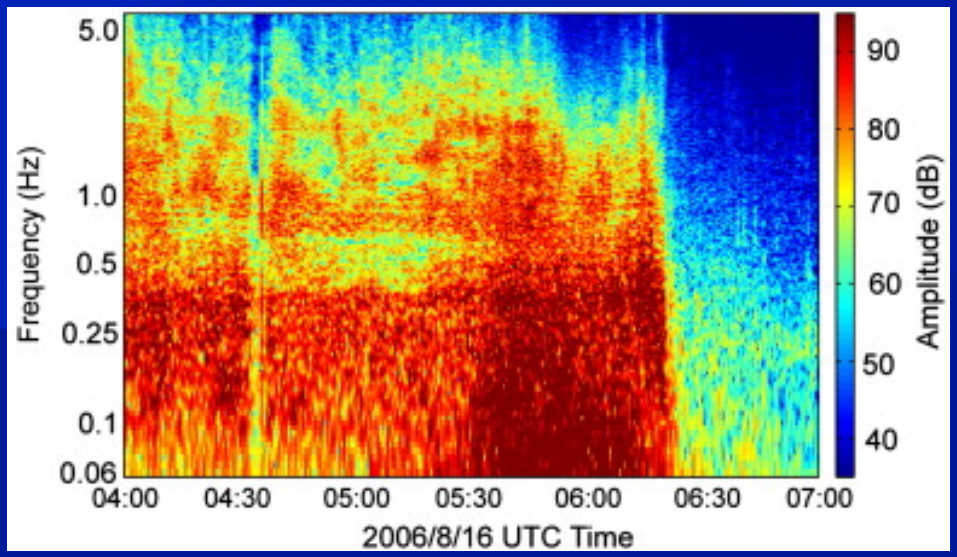

16 August 2006 spectrogram between 0400 and 0700 UTC. Dominant frequency of the jetting shifts to a lower frequency after ~ 0530, coinciding with a Plinian ash column. The eruption ends at ~ 0620.

Acoustic energy calculated in hour-long octave bands. Large amount at low frequency during peak in event

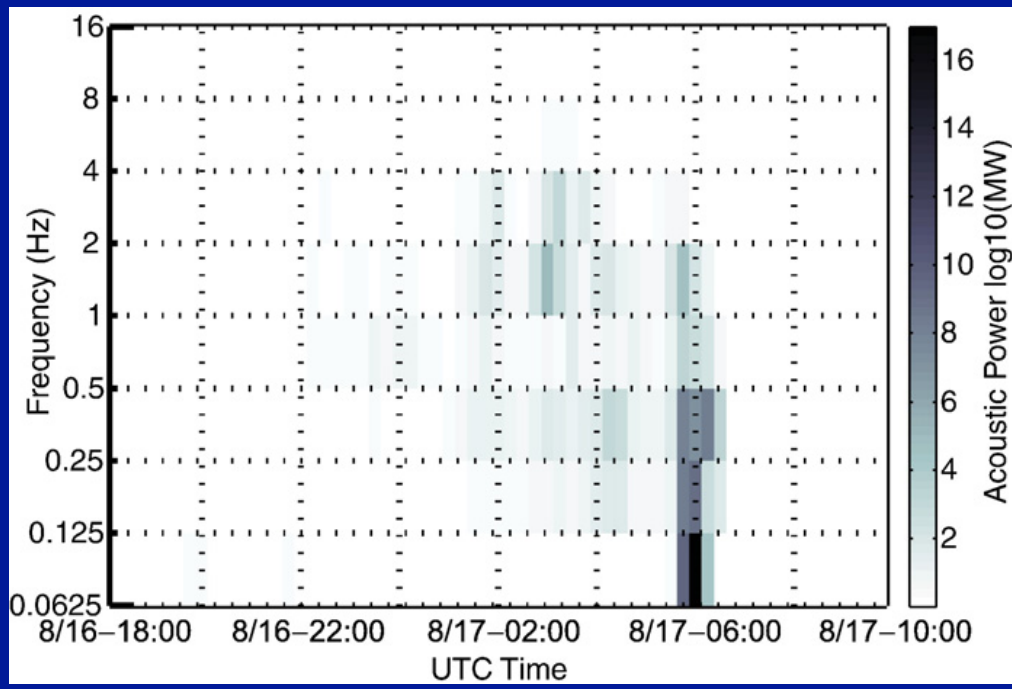

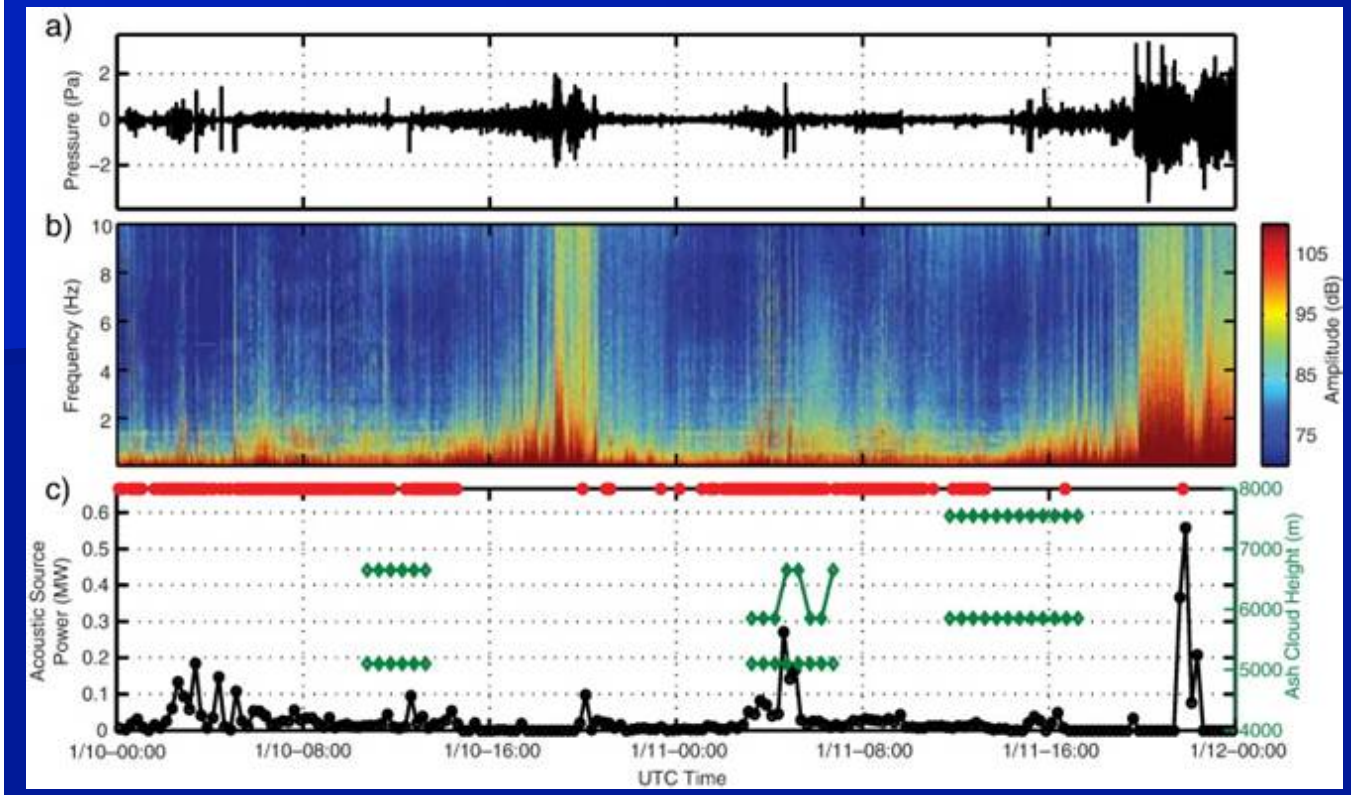

10–11 January 2008

a) raw waveform

b) Spectrogram

c) Acoustic power (black line), column height and detected explosions (red dots).

Numerous Strombolian–type explosions (32/hr), no significant ash plumes were detected. Wind noise dominates the spectrogram during ~ 1900–2300 UTC.

- Acoustic energy from sustained, energetic eruptive activity broadly scales with ash height and has a characteristic spectrum resembling a low-frequency form of jet noise
- During Plinian phase August 2006 eruption, the jet noise spectrum shifted to low frequencies (below 0.1 Hz) and produced over 50MW of acoustic power
- Tool to study dynamics of a variety of eruption styles

Differences between Vulcanian and Strombolian explosions

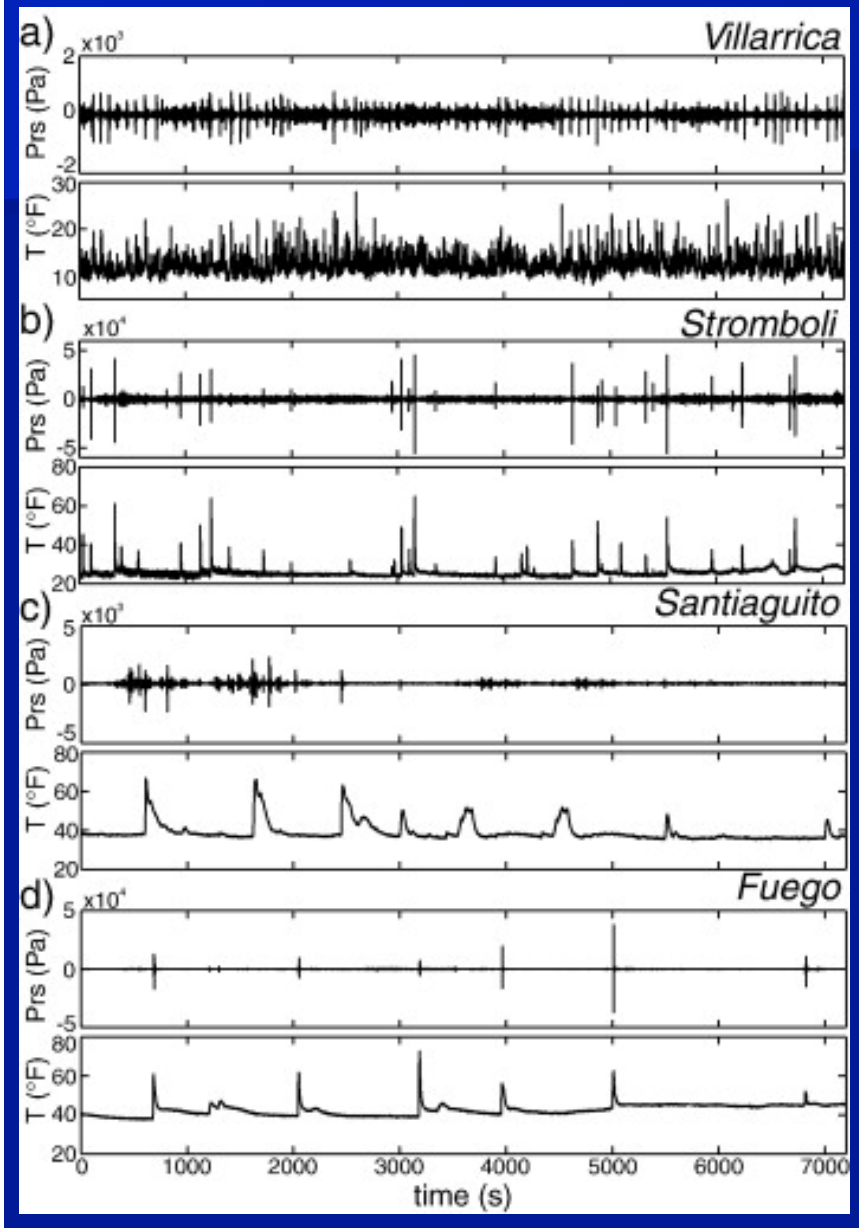

Marchetti et al. 2009. EPSL 279.

2 hr-long samples of infrasonic and thermal records of explosive activity

Infrasound is directly related to the emission of over-pressurized gas
-reflects the plume emission
Both plume emission and ascent are detected thermally.

2 data sets together provide a complete description of the plume dynamics

Stacking of events

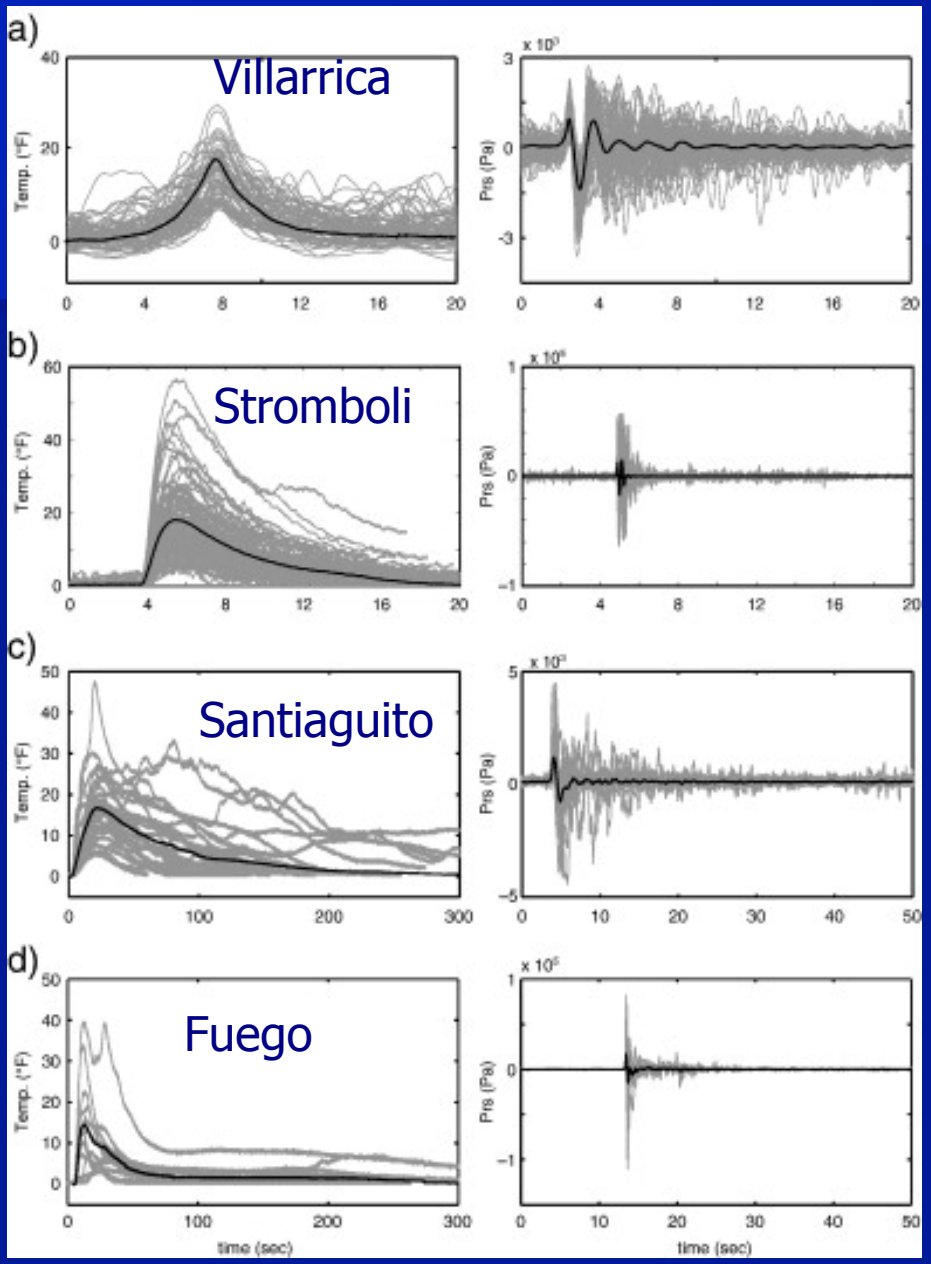

Thermal Infrasonic

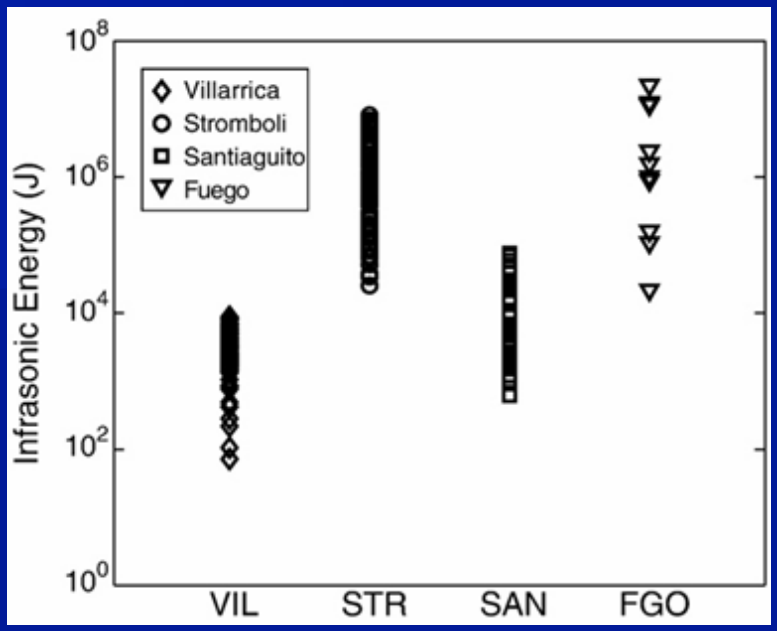

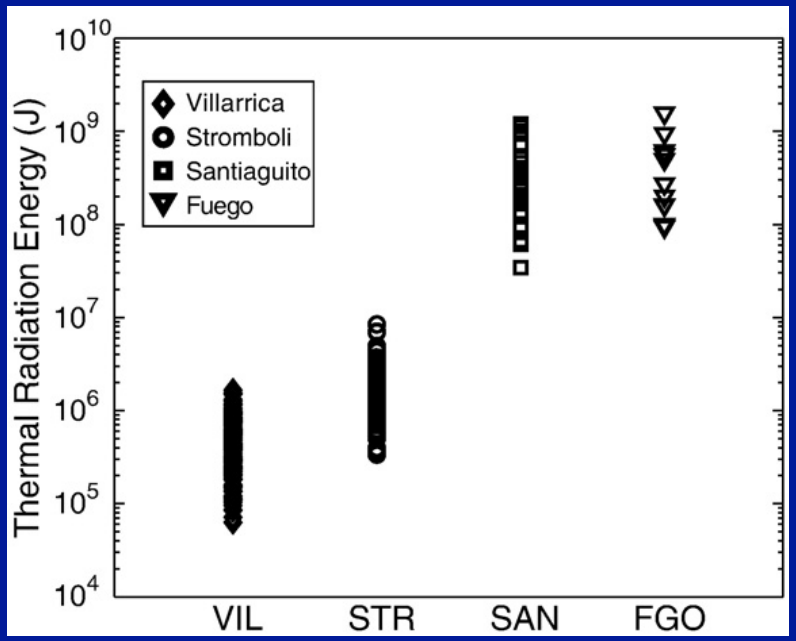

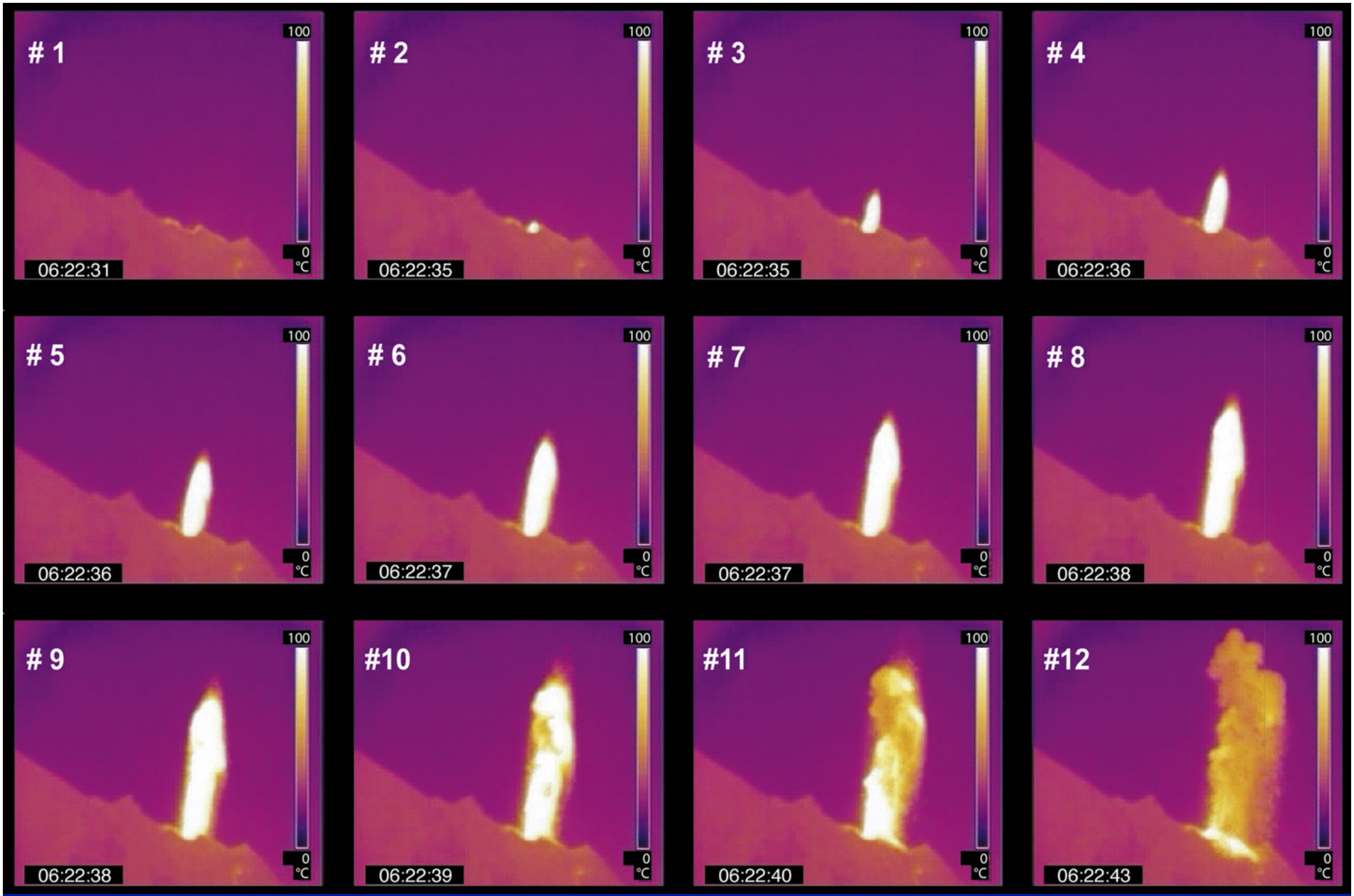

Typical Strombolian explosion at Stromboli thermal camera 450 m from the summit crater. Characterized first by a finger-type jet (frames #1 to #7) which evolves into a buoyant rising cloud (frames #8 to #12).

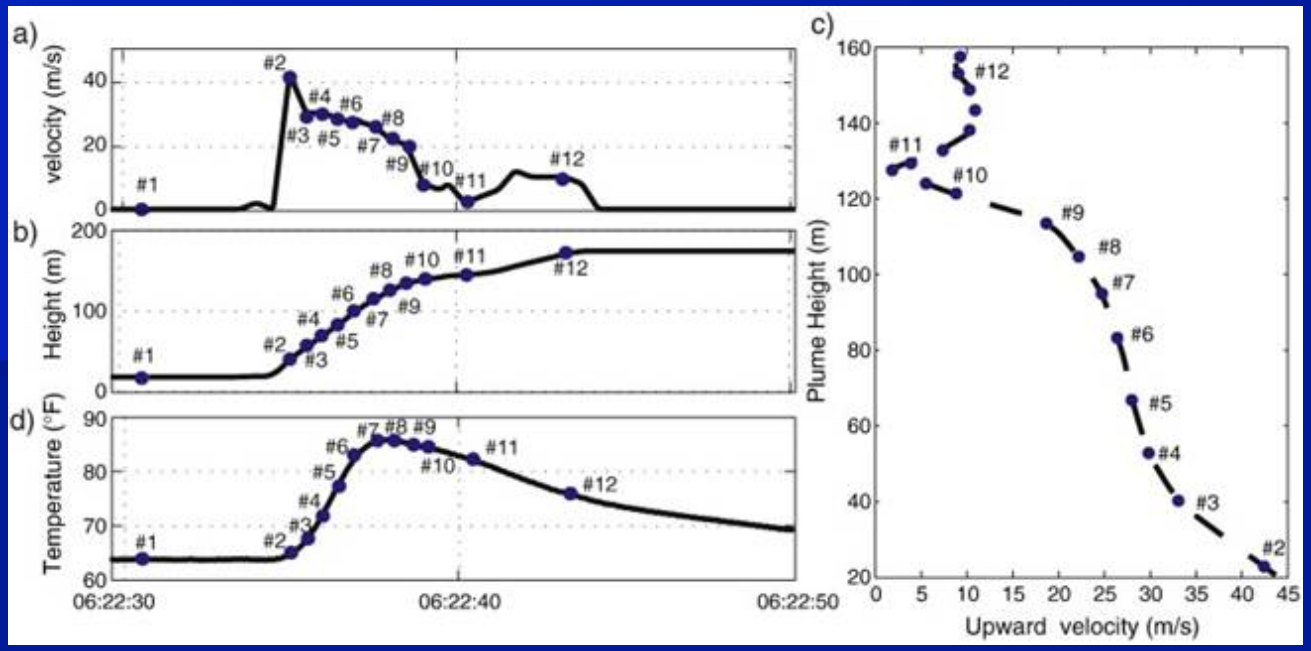

Plume height - continuous increase through time

Velocity reaches the highest value at the initial stage, then constant decrease until frame #10 and is stable afterwards.

Plume evolution - 2 distinct phases, initial rapid deceleration with increasing height up to 120 m (frames #2 to #10) is followed by constant velocity (frames #10 to #12), in ascent driven by an initial gas-thrust followed by buoyancy.

Apparent temperature - asymmetrical shape: first rapid increase - frames #2 to #8
Then longer-lasting decrease - frames #9 to #12.

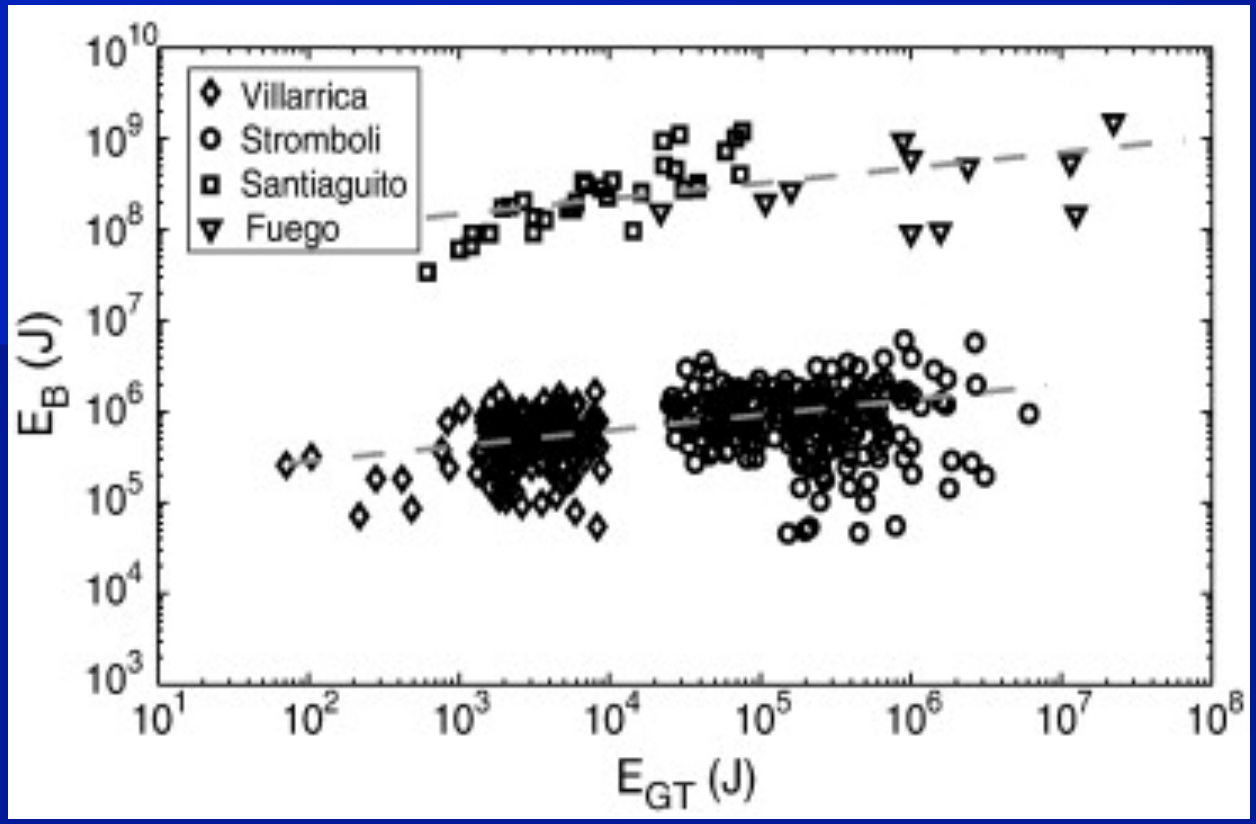

Energy balance for explosions recorded at the 4 case study volcanoes

2 separate clusters of events:
Fuego and Santiaguito - large values of EB
Stromboli and Villarrica - lower EB

Within each cluster buoyancy has a limited increase with gas-trust, following a linear trend (grey dashed lines) with slope of ~ 0.17 common to both clusters.

Large difference in buoyancy reflects 2 different eruptive dynamics producing material with different grain size

Little variation for each volcano – rapid cooling dominating

Integration with Doppler radar – relative mass flux rates at Stromboli

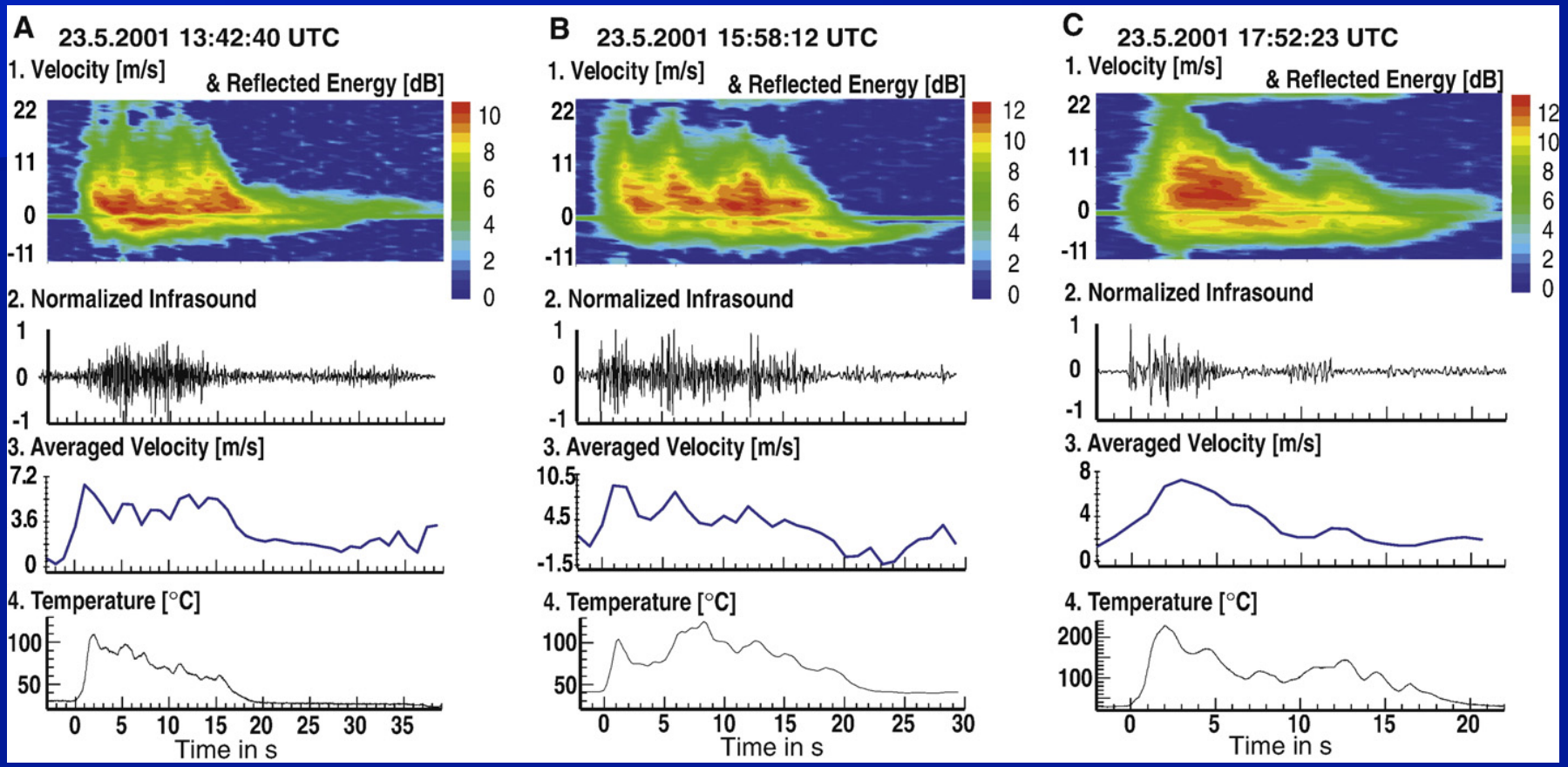

Scharff et al. JVGR 2008

- Good correlation between mass flux inferred from Doppler radar and temperature measurements
- Lack of correlation between acoustic energy & velocity

Onset of the 2007 Stromboli effusive eruption

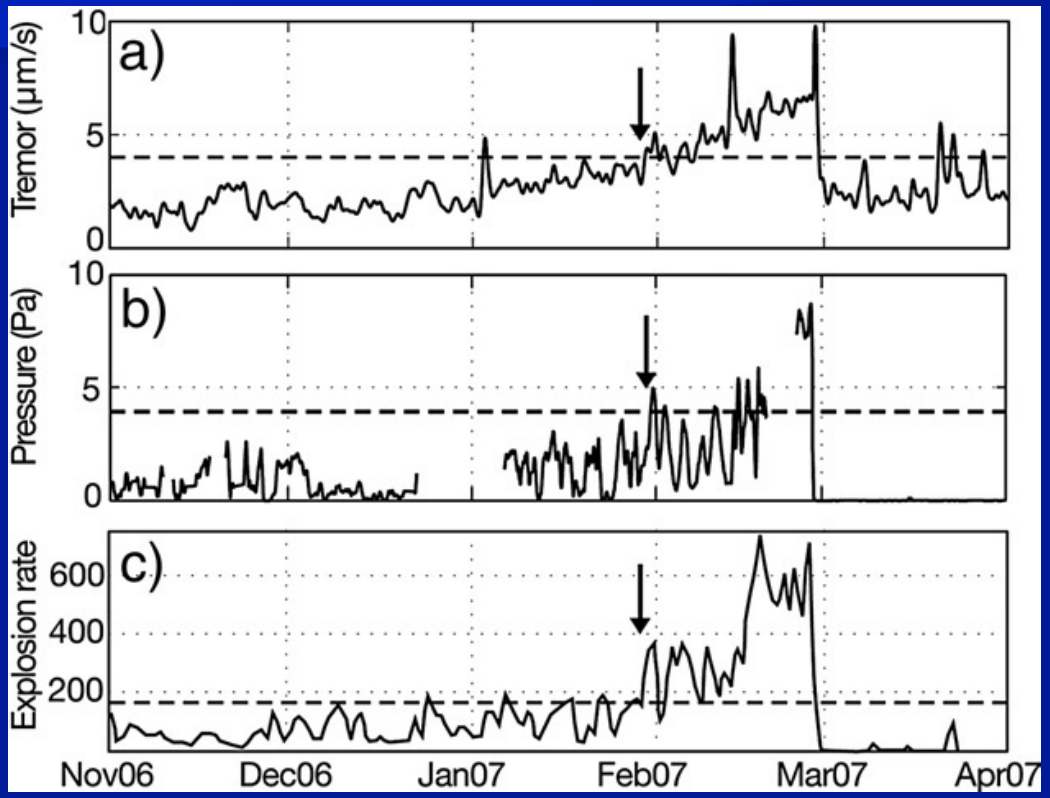

- Seismo-acoustic data integrated with thermal camera, tiltmeters
- (a) Seismic tremor, (b) infrasonic pressure related to degassing activity and (c) number of explosions/day, as revealed by thermal camera
- All the monitored parameters reached the maximum threshold level at the end of January (arrows) almost 1 month before the eruption onset

Ripepe et al. JVGR 2009

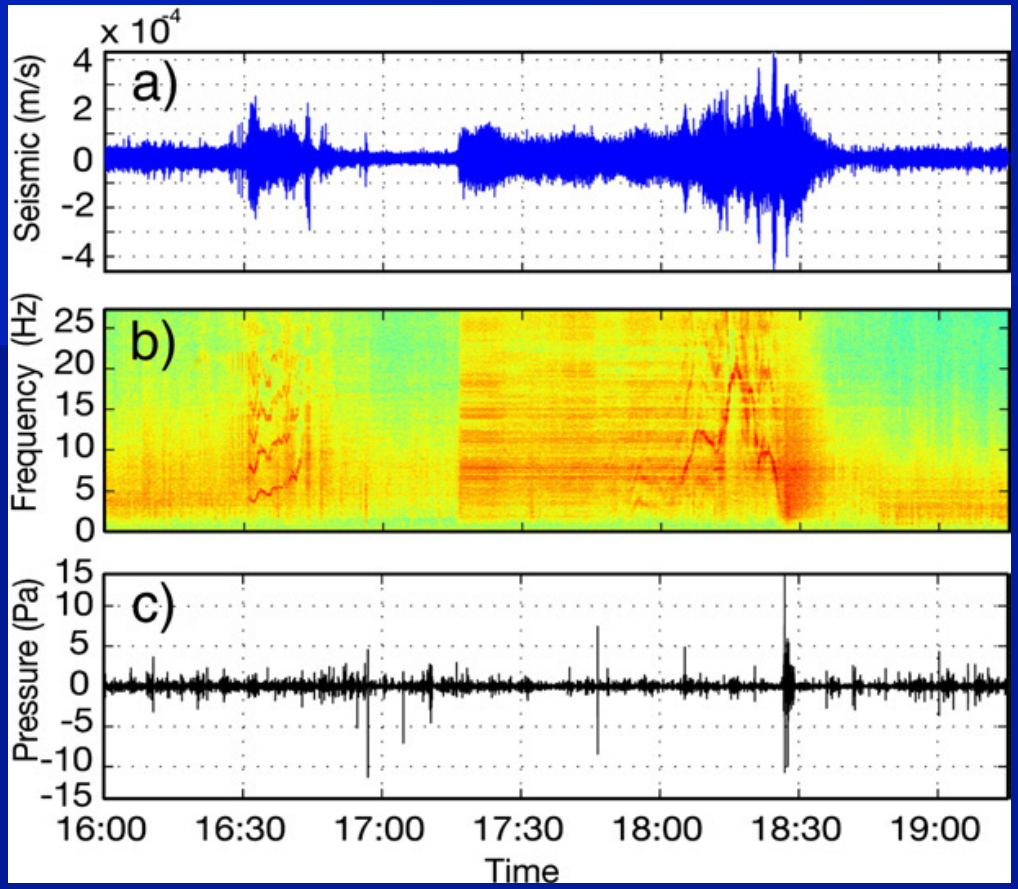

a) High-amplitude phase of tremor

b) Spectrogram showing the high-frequency content with 2 episodes of spectral gliding. The second episode features a frequency content largely above the normal

c) Infrasonic signal detected at 18:26 GMT by the array located in the Sciara del Fuoco - landslide associated with the opening of the lateral effusive vent at 400 m of elevation

High-amplitude and high-frequency harmonic tremor occurred during a non-explosive phase of the summit craters, and seems directly related to the opening of the effusive vent.

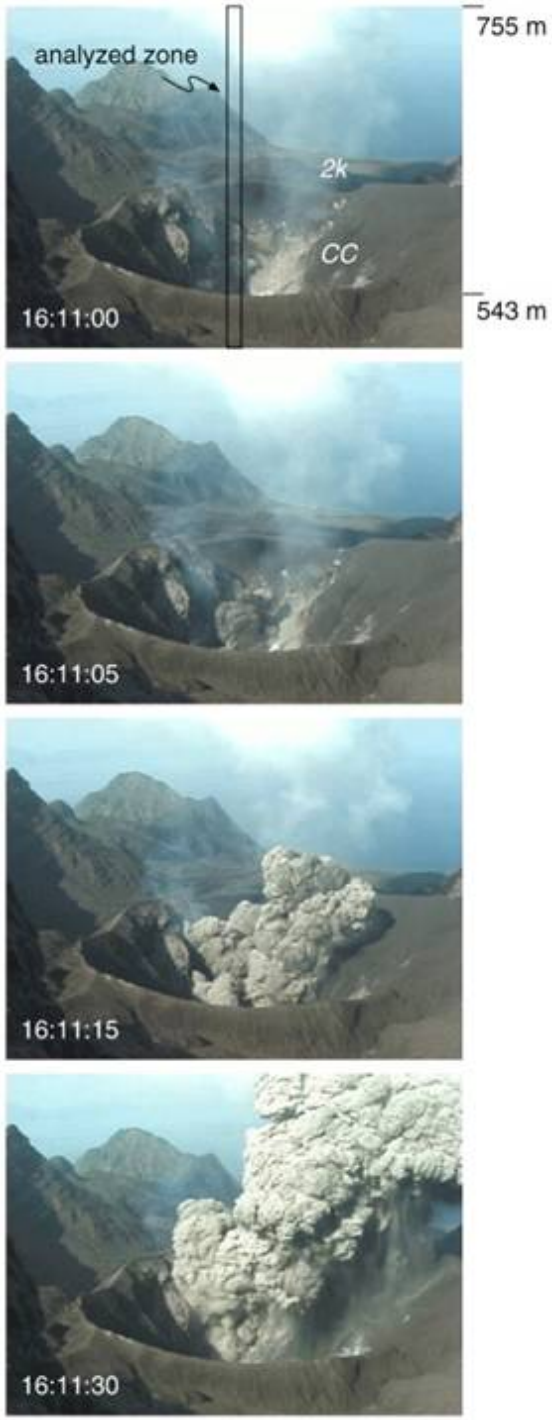

Infrasound generation at Suwanosejima

- Just before the eruption onset, only dilute steaming gas was visible above the crater
- At 16:11:02, the first volcanic cloud (jet) suddenly appeared
- Ballistics were subsequently ejected for ~20 min.

Yokoo et al. JVGR 2010

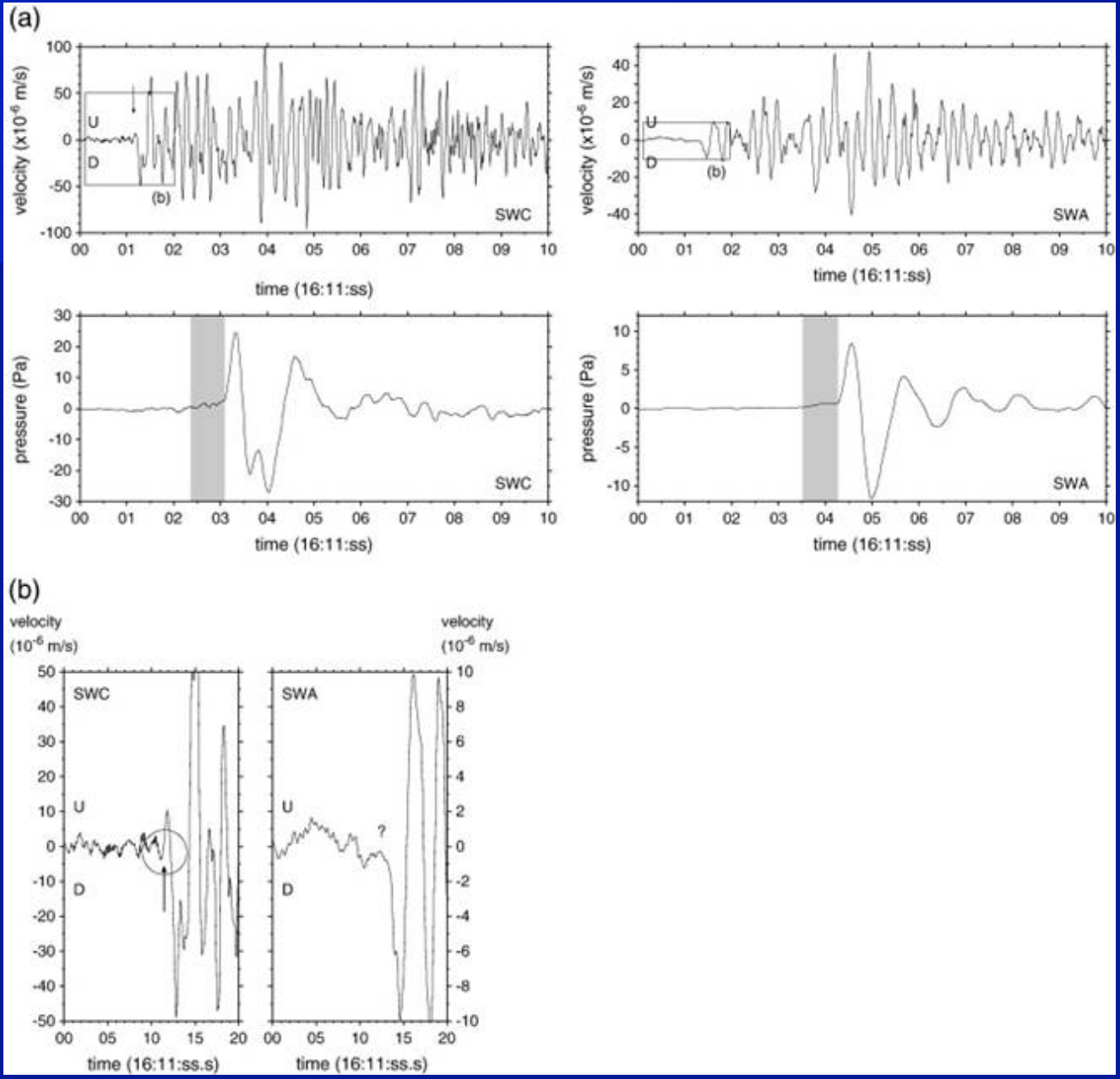

(a) Seismic and infrasound signals associated with the 16:11 eruption Arrow in the seismogram of SWC denotes the arrival time of the P-wave.

Grey-coloured periods in the infrasound records denote the preceding phases followed by the main compression phases.

(b) The initial part of each seismogram at SWC and SWA.

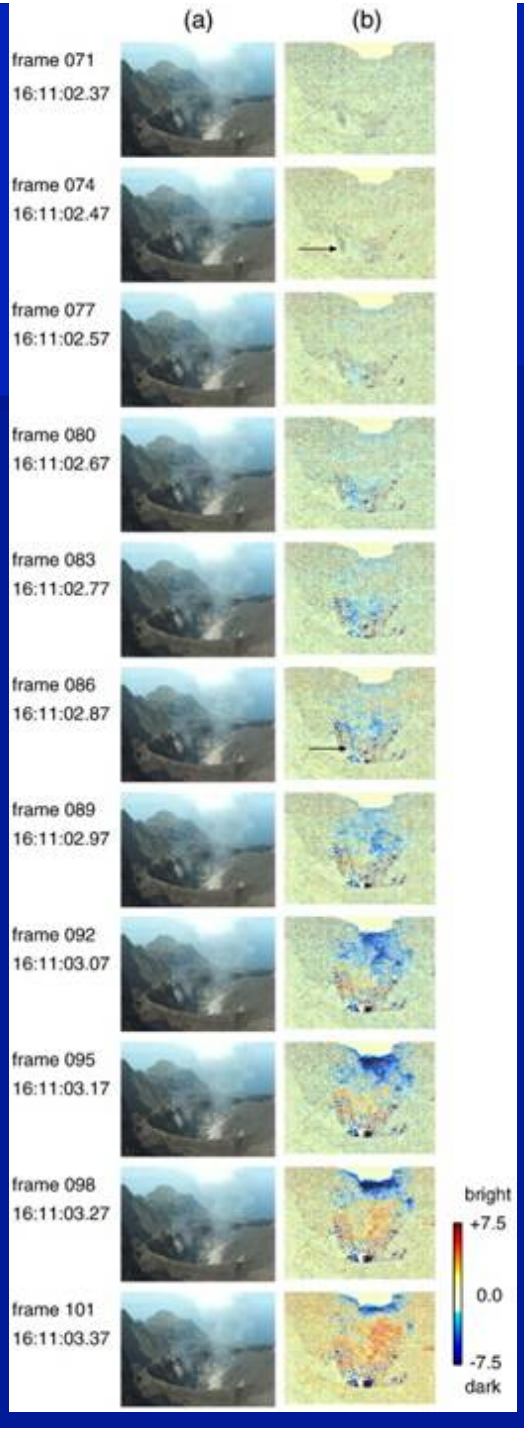

Temporal change in the luminance data

Increase in luminance is represented as a colour change from blue to red - seen mainly in the area where steam emerges from the crater

Around frame 74 (16:11:02.47), a bluish cluster begins to travel upward from the bottom in the images, followed by a reddish area beginning at frame 86 (16:11:02.80)

This first decrease in luminance represents a weak phase change of H_2O from steam to vapour, and the subsequent brightening represents vapour reverting back to steam.
Caused by propagation of an air pressure wave generated by the eruption as observed in the infrasound waveforms.

At the 101st frame (16:11:03.37), almost the entire image is coloured red, suggesting that pressure wave was propagating hemispherically outward into the surrounding space

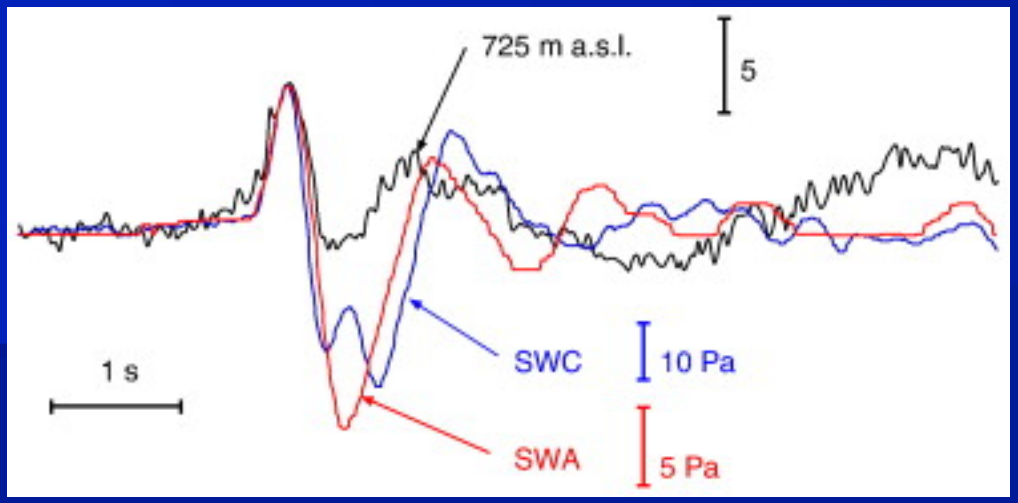

Comparison of corrected luminance change at 725m a.s.l. (black line) and observed pressure changes

Initial part of the 16:11 eruption at Suwanosejima volcano

a) At almost the same time that the onset of vertical expansion occurred at ~0.5 km depth, swelling of the crater bottom began, which produced the preceding phase of the infrasound wave

(b) Ejection of volcanic cloud began with the main phase of infrasound radiation about 0.7 s after the start of swelling.